MATERIALS CHEMISTRY FRONTIERS

Generating a three-dimensional non-fullerene electron acceptor by combining inexpensive spiro[fluorene-9,9'-xanthene] and cyanopyridone functionalities

Journal:	*Materials Chemistry Frontiers*
Manuscript ID	QM-RES-02-2018-000067.R1
Article Type:	Research Article
Date Submitted by the Author:	21-Mar-2018
Complete List of Authors:	Kadam, Gajanan; North Maharashtra University, Pree, Anuradha; RMIT University, School of Science Agarwal, Anubha ; Deakin University - Geelong Waterfront Campus, institute for frontier material Puyad, Avinash; S.R.T.M. University, School of Chemical Sciences La, Duong; RMIT university, Applied Sicences Evans, Richard; CSIRO , Materials Science and Engineering; Li, Jingliang; Deakin University, Institute for Frontier Materials Gupta, Akhil; Monash University, Department of Materials Engineering, Faculty of Engineering Bhosale, Sheshanath; RMIT University, Department of Chemistry; Goa University, Department of Chemistry

Journal Name

ARTICLE

Generating a three-dimensional non-fullerene electron acceptor by combining inexpensive spiro[fluorene-9,9'-xanthene] and cyanopyridone functionalities

Received 00th January 20xx,
Accepted 00th January 20xx

DOI: 10.1039/x0xx00000x

www.rsc.org/

Gajanan Kadam,[a] Anuradha.,[b] Anubha Agarwal,[c] Avinash Puyad,[d] Duong Duc La,[b] Richard A. Evans,[e] Jingliang Li,[c] Akhil Gupta*[c] and Sheshanath V. Bhosale*[f]

Through the combination of cheaply synthesized structural fragments, spiro[fluorene-9,9'-xanthene] – otherwise termed low-cost spiro – and cyanopyridone, herein we report a new, three-dimensional, small molecule non-fullerene electron acceptor, (5*Z*,5'*Z*,5''*E*,5'''*E*)-5,5',5'',5'''-((((*S*)-spiro[fluorene-9,9'-xanthene]-2,2',7,7'-tetrayl)tetrakis(thiophene-5,2-diyl))tetrakis(methaneylylidene))tetrakis(4-methyl-1-octyl-2,6-dioxo-1,2,5,6-tetrahydropyridine-3-carbonitrile) [**A1**], which was synthesized for use in solution-processable bulk-heterojunction devices and was fully characterized by proton and carbon NMR spectroscopies together with elemental analysis. **A1** was synthesized by a facile synthetic methodology using a Knoevenagel condensation reaction and was found to be highly soluble in a variety of common processing solvents such as chloroform and *o*-dichlorobenzene. Owing to its envisioned design, **A1** displayed promising optoelectronic properties, and energy levels complementing those of the conventional donor polymers poly(3-hexylthiophene) [P3HT] and Poly({4,8-bis[(2-ethylhexyl)oxy]benzo[1,2-*b*:4,5-*b'*]dithiophene-2,6-diyl}{3-fluoro-2-[(2-ethylhexyl)carbonyl]-thieno[3,4-*b*]thiophenediyl}) [PTB7]. Given its energy levels, solubility and excellent film forming capability, **A1** was used in bulk-heterojunction devices as an *n*-type semiconducting component. The device performances [D: A 1: 1.2 = 5.84% (P3HT); 7.21% (PTB7)] validated the design and use of **A1** as an efficient non-fullerene acceptor.

1. Introduction

The development of renewable energy technologies based on harvesting solar energy at an affordable price is a pressing need for society. The technologies such as organic (otherwise termed bulk-heterojunction) solar cells are highly promising given the advantages, such as lightweight, flexibility and low-cost, they offer.[1–4] The development of such devices has seen advancements in the areas of new material design and fabrication strategies. In terms of materials development, donor and acceptor materials have been extensively researched. The conventional donor-acceptor material combinations, such as donor polymer poly(3-hexyl thiophene) (P3HT) and soluble fullerene acceptors, [6,6]-phenyl-C_{61}-butyric acid methyl ester ($PC_{61}BM$) and its C_{71} analogue ($PC_{71}BM$), have been thoroughly studied to understand device design, morphological controls, and consistent device outcome. Despite the achievement of high conversion efficiencies using fullerene acceptors, non-fullerene acceptors have been developed over the past few years as they are seen to possess multiple advantages beyond their fullerene-based counterparts, such as strong light harvesting, easily tunable energy levels, improved morphological stability, and facile synthetic manipulations.[5–12]

Although the fullerene acceptors provide a number of advantages, such as good electron mobility, excellent solubility and the ability to form a favourable nanoscale network with donor semiconducting components, they are afflicted with a number of limitations, e.g. poor chemical and electronic tunability, weak absorption in the visible region, and a large electron affinity that results in low open-circuit voltage.[13] Fullerenes are also expensive, thus making their mass uptake challenging. These disadvantages of fullerenes encourage researchers to develop non-fullerene acceptors that can compete with fullerene acceptors by retaining properties, such as strong accepting strength, solubility, and thermal stability, but adding the ability to tune energy levels and scalable synthetic routes. Therefore, the design and development of a potential non-fullerene acceptor based on such requirements is an important and worthy challenge for both organic chemists and device physicists.

a Department of Organic Chemistry, School of Chemical Sciences, North Maharashtra University, Jalgaon 425001 Maharashtra, India
b School of Science, RMIT University, GPO Box 2476, Melbourne, Victoria 3001, Australia
c Institute for Frontier Materials, Deakin University, Waurn Ponds, Victoria 3216, Australia. E-mail: akhil.gupta@deakin.edu.au; Tel: +61 3 5247 9542; orcid.org/0000-0002-1257-8104
d School of Chemical Sciences, Swami Ramanand Teerth Marathwada University, Nanded 431606, Maharashtra, India
e CSIRO Manufacturing, Bayview Avenue, Clayton South, Victoria 3169, Australia
f Department of Chemistry, Goa University, Taleigao Plateau, Goa 403206, India. Email: svbhosale@unigoa.ac.in; bsheshanath@gmail.com Tel: +91 (0866) 9609303; orid.org/0000-0003-0979-8250
Electronic Supplementary Information (ESI) available: [DFT calculations, computed absorption, PESA, TGA, XRD, and experimental spectra]. See DOI: 10.1039/x0xx00000x

It is evident from the recent literature that several structural types, including small molecules and conjugated polymers, have been developed as efficient non-fullerene electron acceptors.[14–28] Among the reported literature, the most recent reports on encouraging efficiencies of bulk-heterojunction (BHJ) devices and unique material design are the reports that comprise of non-planar, three-dimensional (3D) structural architecture. Such non-planar molecular arrangements can reduce electronic coupling and charge recombination,[29] provide high thermal stability, and favourable solubility. Moreover, such formats can prevent strong intermolecular aggregation, whilst sustaining extended and effective conjugation in each direction for superior photon harvesting. One of the key methods to achieve such properties and a 3D architecture is the utilization of a structural format that can be used centrally and allows multiple functionalities to be placed at its peripheries. The structures like 9,9'-spirobi[fluorene],1,1,2,2-tetraphenylethene and 9,9'-bifluorenylidene are the principal blocks that have been reported in the recent literature to generate 3D architectures. Reviews by H.-W. Luo *et al.*, N. Liang *et al.* and W. Chen *et al.* provide such details[30–32] and indicate that there is still a large scope for those structural units which can be employed to generate non-planar targets.

To overcome the high cost and synthetic complexity of the literature reported units, however, in the present study, we have focussed our intention on spiro[fluorene-9,9'-xanthene] (SFX), which is a cheaply synthesized unit and is reported as a "low-cost spiro" by M. Maciejczyk *et al*.[33] This unit has further been reported to produce eco-friendly green organic semiconductors, such as organic light emitting diodes (OLEDs),[34] and more recently, perovskite solar cells.[30–32,35] Surprisingly, among the reported literature, no derivatives have been described that can be used as non-fullerene acceptors. An additional motivation for our interest in the design of a novel, 3D target molecule based on SFX was the recent success that we were able to achieve using cyanopyridone as a terminal accepting group.[36,37] Taking into account the advantages exhibited by cyanopyridone, such as strong accepting strength, low-cost synthesis and capability to be placed at terminals, together with the literature precedence, herein we report the very first combination of SFX and cyanopyridone functionalities to generate a novel, 3D small molecule non-fullerene electron acceptor, (5*Z*,5'*Z*,5''*E*,5'''*E*)-5,5',5'',5'''-((((*S*)-spiro[fluorene-9,9'-xanthene]-2,2',7,7'-tetrayl)tetrakis(thiophene-5,2-diyl))tetrakis(methaneylylidene))tetrakis(4-methyl-1-octyl-2,6-dioxo-1,2,5,6-tetrahydropyridine-3-carbonitrile), **A1** (Fig. 1). The new target **A1** was synthesized *via* a Knoevenagel condensation reaction between 5,5',5'',5'''-(spiro[fluorene-9,9'-xanthene]-2,2',7,7'-tetrayl)tetrakis(thiophene-2-carbaldehyde) and cyanopyridone (Scheme 1; Experimental section). The reaction protocol was very simple and was carried out in methanol at reflux for 24 h. The structure of **A1** was confirmed by ^{1}H and ^{13}C NMR spectroscopies, MALDI-TOF and elemental analysis (for experimental spectra see Electronic Supplementary Information (ESI)). The molecule **A1** was found to be highly soluble in most of the routinely used laboratory solvents, e.g. chlorobenzene, chloroform and *o*-dichlorobenzene, a prerequisite for fabricating solution-processable BHJ devices. Our idea of designing **A1** as a non-fullerene acceptor was validated as the solution-processable BHJ devices comprising two different commercially available donor polymers, poly(3-hexylthiophene) [P3HT] and poly({4,8-bis[(2-ethylhexyl)oxy]benzo[1,2-*b*:4,5-*b*']dithiophene-2,6-diyl}{3-fluoro-2-[(2-ethylhexyl)carbonyl]-thieno[3,4-*b*]thiophenediyl}) [PTB7], afforded very encouraging and high device outcome [(P3HT: **A1** 1: 1.2 = 5.84%); (PTB7: **A1** 1: 1.2 = 7.21%)]. Not only is **A1** the first reported example in the literature where a unique combination of cheaply synthesized building blocks, SFX and cyanopyridone, has been carried out, but the device outcome reported herein is among the reasonable and encouraging efficiencies, apart from the class of ITIC-based acceptors,[23–25] that has been achieved using a simple device architecture and without any special treatment to either blend solution or to the overall device. This work confirms the idea that 3D structural formats are highly efficient non-fullerene acceptor architectures that hold a strong promise for organic photovoltaic (OPV) research. The current work is a continuation of our efforts made in the design and development of small molecule chromophores for OPV applications.[38–40]

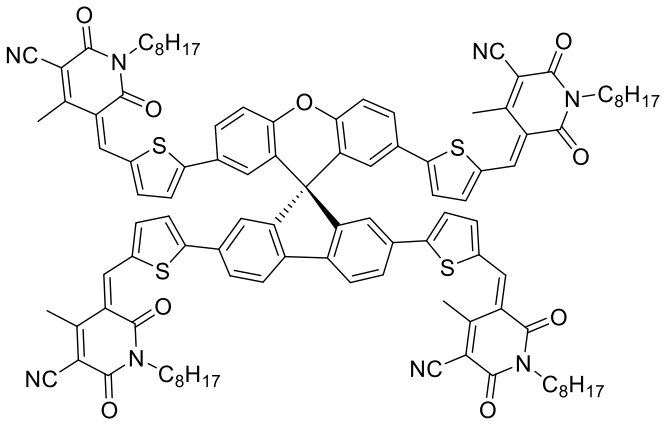

Fig. 1 Molecular structure of the newly designed and synthesized non-fullerene acceptor **A1**.

2. Results and discussion

The normalized optical absorption spectra of **A1** in chloroform solution, and as a thin solid and blend films are shown in Fig. 2. In solution, **A1** exhibited strong absorption with an absorption maximum (λ_{max}) at 518 nm (molar extinction coefficient = ~52, 000 L Mol^{-1} cm^{-1}). The thin film spectrum of **A1** was red-shifted by 10 nm when compared with its solution spectrum. The blend film spectra of **A1** (with P3HT and PTB7) indicated strong light-harvesting ability, and in particular with PTB7 where the pristine film absorption of **A1** complemented very well with the absorption profile of PTB7, thus suggesting that blend film has promising absorption over whole of the visible region. This further confirms that the use of a narrow band-gap donor polymer like PTB7 is indeed helpful for (1) fine tuning energy levels, (2) exhibiting favourable and well-intermixed blend

morphology, and (3) presumably enhancing BHJ performance when compared with a wide band-gap donor polymer P3HT.

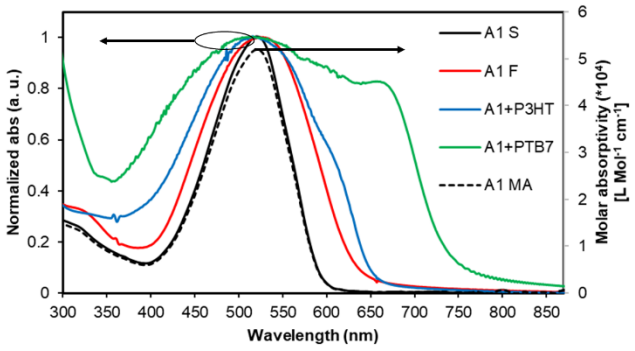

Fig. 2 The UV–Vis absorption spectra of **A1** in chloroform solution (**A1** S), as a pristine film (**A1** F), and as a blend with P3HT (**A1** + P3HT) and PTB7 (**A1** + PTB7) [1: 1.2 (*w*/*w*)]. The molar absorptivity is represented by a dotted black curve (**A1** MA; Y-axis).

In order to obtain information about the theoretical density distribution of **A1**, the Gaussian 09 ab initio/DFT quantum chemical simulation package was employed to acquire results represented in the present work.[41] The geometry optimization of **A1** with truncated alkyl chains was carried out at the B3LYP/6-31G(d) level of theory and the frontier molecular orbitals (FMOs) were generated using Avogadro[42,43] (for details on DFT calculations, see Table S1 and Fig. S1, ESI). The DFT calculations indicated that the lowest unoccupied molecular orbital (LUMO) and the highest occupied molecular orbital (HOMO) orbital densities were evenly dispersed over the entire molecular backbone, a recent finding that is quite common with high-performing, small-molecule non-fullerene electron acceptors.[15,16,44] Furthermore, in order to understand the nature of charge transfer transition, we conducted time-dependent DFT calculations (TD-DFT). The TD-DFT calculations provide excitation energies and oscillator strengths (denoted by f) of the lowest singlet states. The computed absorption spectrum (see Fig. S2, ESI) shows transition peaks at 539 nm and 512 nm, with the former peak mainly described as the HOMO/LUMO transition (H → L = 95%). Consequently, the subsequent analysis of the transition density matrix *via* natural transition orbitals (NTOs) produces a pair of NTOs with a very similar character as the corresponding HOMO/LUMO pair (see Fig. S3, ESI). The experimental estimation of the HOMO was carried out using photo electron spectroscopy in air (PESA) and the LUMO energy level was calculated using the method reported by P. I. Djurovich *et al.*[45] (for PESA curve, see Fig. S4, ESI). The HOMO (-5.81 eV) and the LUMO (-3.78 eV) values are depicted in the energy level diagram (see Fig. S5, ESI), which indicates that the energy levels of **A1** are complementing excellently with the energy levels of two different types of donor polymers, P3HT and PTB7. The energy levels' alignment indicates that the devices comprising standard donor polymers and **A1** indeed guarantee a high open-circuit voltage (V_{oc}), which is certainly advantageous, when compared with the devices incorporating the conventional fullerene acceptor. We further realized that the organic semiconductors, whether donors or acceptors, should also be thermally stable so that they can handle tough fabricating conditions, e.g. annealing at a higher temperature such as 100 °C. Keeping this criterion in mind, we conducted thermogravimetric analysis (TGA). The TGA analysis revealed that **A1** is a thermally stable chromophore and the organic solar cell device incorporating **A1** can be well annealed, if required. For TGA spectrum, see Fig. S6, ESI.

Once it was established that **A1** is adequately soluble in a variety of common organic solvents, is thermally and chemically stable, and has energy levels compatible with those of donor polymers, P3HT and PTB7, we fabricated solution-processable BHJ devices using **A1** as a non-fullerene acceptor. Though we realised that the pristine and P3HT blend film spectra of **A1** are somewhat similar, we still chose to fabricate BHJ devices using P3HT. This was primarily done to realise the potential of **A1** with the historic benchmark polymer and to understand its exciton dissociation efficacy. That being said, we expected the outcome of P3HT-based devices to be inferior when compared with PTB7-based devices given latter's complementary absorption with **A1**. Considering the efficacy of **A1** as an acceptor and its proposed testing with two different donor polymers, we chose a simple device architecture, indium-tin oxide (ITO)/poly(3,4-ethylenedioxythiophene):polystyrene sulfonate (PEDOT:PSS, 38 nm)/active layer (~70 nm)/Ca (20 nm)/Al (100 nm), where the active layer was a 1: 1.2 blend of P3HT/PTB7: **A1**, respectively, spin-cast from *o*-dichlorobenzene atop PEDOT:PSS surface. Taking an advantage of the literature findings and our own understanding of the BHJ device architecture, we used a high boiling point solvent and annealed our active surfaces at 110 °C for five minutes. We also fabricated control devices based on P3HT: $PC_{61}BM$ combination. With the PTB7: **A1** combination, the device outcome was highly encouraging and the cell parameters; V_{oc}, short-circuit current density (J_{sc}), fill factor (*FF*) and power conversion efficiency (PCE), reached 1.04 V, 11.01 mA cm^{-2}, 0.63, 7.21%, respectively. With P3HT combination, the achieved device parameters, V_{oc}, J_{sc}, *FF* and PCE, were 1.01 V, 9.56 mA cm^{-2}, 0.61, and 5.84%, respectively. Both of the devices achieved high open-circuit voltages as was predicted from the energy level diagram. This is consistent with the measured LUMO level of **A1** and the HOMO levels of donor polymers. The unannealed devices with a similar donor: acceptor weight ratio provided satisfactory outcome too and the PCE values reached to 4.50% and 4.13% with PTB7 and P3HT, respectively. In contrast, the maximum PCE reached 3.03% for a controlled device based on P3HT:$PC_{61}BM$. For current–voltage (*J*–*V*) curves and detailed device parameters, see Fig. 3 and Table S2, ESI, respectively.

The PTB7-based devices clearly outperform devices based on P3HT under alike conditions. The improvement is mostly due to an increase in the short-circuit current density, a finding that is consistent with the broader blend film absorption of PTB7 and **A1**. A similar pattern was observed for the incident photon-to-current conversion efficiency (IPCE) measurement where a much broader and stronger response was observed for PTB7-based devices when compared with P3HT-based devices, see Fig. 4 for IPCE spectra. The IPCE maxima of 64% (at 570 nm) and 48% (at 550 nm) were attained for PTB7- and P3HT-based devices, respectively. Though the broadness of these spectra

indicated that both donor and acceptors components in active blends made a considerable contribution to the IPCE and J_{sc}, the PTB7-based spectrum spanned over most of the visible region,

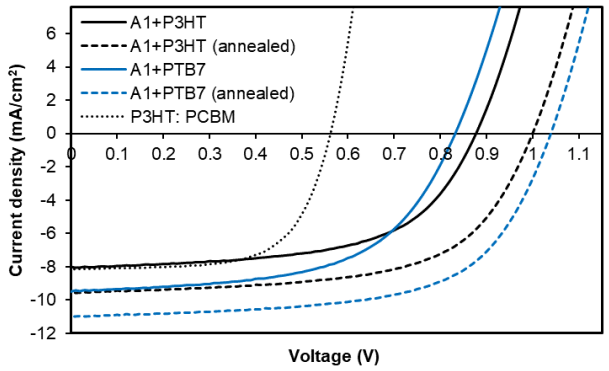

Fig. 3 Characteristic current–density *vs.* voltage (*J–V*) curves for the best BHJ devices based on **A1** in blends with PTB7 and P3HT. Solid and dashed black lines correspond to pre-annealing and post-annealing conditions, respectively, under simulated sunlight (100 mW cm^{-2} AM 1.5G); blend ratio = 1: 1.2 *w/w* (D/A). Device structure was: ITO/PEDOT: PSS (38 nm)/active layer (~70 nm)/Ca (20 nm)/Al (100 nm).

typically ranging 350 nm to 820 nm, thus suggesting better light-harvesting and a superior blending of donor and acceptor domains. Furthermore, the photocurrents obtained from the IPCE data were in close agreement with those of the current–voltage measurements conducted under the one Sun condition. The high-quality intermixing of donor and acceptor domains in case of PTB7 blend was further confirmed by atomic force microscopy (AFM) analysis, which was conducted in tapping mode, where a much smoother surface with more desirable morphology was observed when compared with P3HT blend. The actual surface morphologies of the blend films of P3HT: **A1** and PTB7: **A1** (1: 1.2 *w/w*) are shown in Fig. 5. The annealed blend surfaces showed surface roughnesses of 1 nm (PTB7: **A1**) and 6.7 nm (P3HT: **A1**), thus suggesting that **A1** is type of non-fullerene acceptor which is highly miscible with a variety of donor polymers, for instance narrow and broad band-gap polymers. The AFM analyses further validated the idea of using a high boiling point solvent as it produced much smoother films which were free from discernible lumps and cracks.

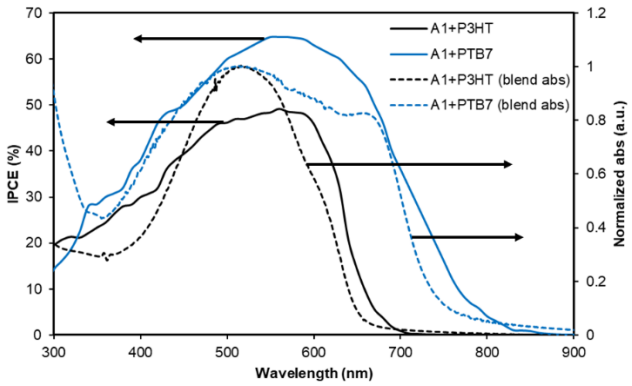

Fig. 4 The IPCE curves of the best performing devices described in Fig. 3. The solid lines correspond to IPCE spectra and the dotted lines represent blend film absorption profiles.

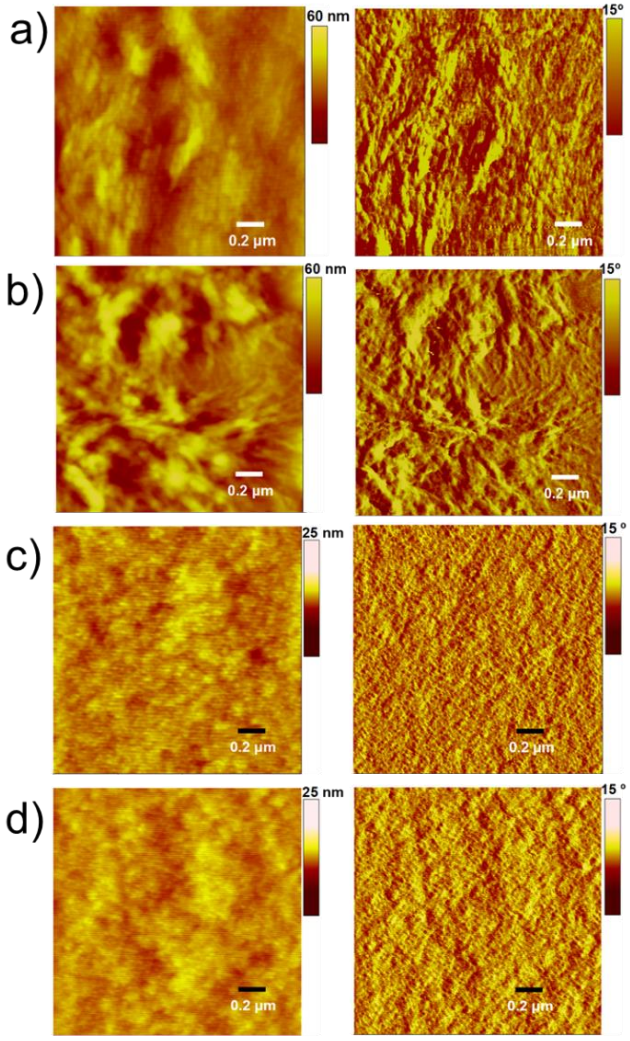

Fig. 5 AFM images for the unannealed and annealed blends of P3HT: **A1** (a and b, respectively) and PTB7: **A1** (c and d, respectively) with the specified weight ratios of 1: 1.2 (D: A). The root-mean square (RMS) roughnesses of 1 nm and 6.7 nm were observed for the annealed blend surfaces of PTB7 and P3HT, respectively.

Furthermore, the transmission electron microscopy (TEM) analysis indicated a fine and featureless appearance that was observed for both the blends (Fig. 6), with the quality of PTB7: **A1** significantly finer than the P3HT: **A1** combination. It is apparent that such uniform and regularized blend surfaces usually result in relatively higher values of J_{sc} and *FF*, as is the case of **A1** blends, and with PTB7 in particular. Furthermore, we conducted the X-ray diffraction (XRD) analysis in order to observe whether the blend surfaces are crystalline or amorphous. Both the blend surfaces were found to be amorphous, thus ruling out the possibility of granular morphologies (for XRD spectra, see Fig. S7, ESI). This indicated that it was the significant miscibility of **A1** with two different types of donor polymers that contributed to the observed device performance. This further validates the design concept used in **A1**, and with the cheaply synthesized building blocks, SFX and cyanopyridone, in particular. The excellent performance of **A1** as a non-fullerene acceptor suggests that other acceptor groups at the terminals will be worth examining.

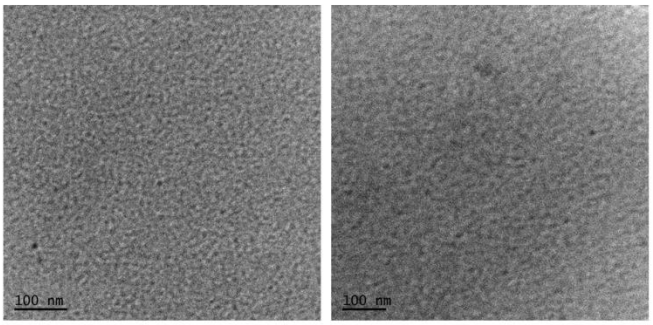

Fig. 6 TEM images for the active blend surfaces of PTB7: **A1** (left) and P3HT: **A1** (right) (D: A 1: 1.2). The PTB7 blend surface seemed much finer when compared with the P3HT blend surface. For a comparative view, identical scale bars of 100 nm are shown.

3. Conclusions

In summary, we were able to design, synthesize and characterize a novel non-fullerene electron acceptor, coded as **A1**, which is a SFX core-based material with terminal cyanopyridone functionalities. **A1** possessed a non-planar molecular arrangement, promising optoelectronic properties, adequate solubility, thermal and chemical stability, and energy levels complementing excellently with two different types of donor polymers, P3HT and PTB7. Due to favourable morphology, excellent blend film characteristics and high J_{sc}, the BHJ devices based on the blended films of PTB7: **A1** provided a PCE of 7.21%. Not only is **A1** the first example in the literature that comprises SFX and cyanopyridone building blocks, but the device parameters outlined herein are among the leading numerals that have been achieved using a simple device design, 3D molecular architecture, and with the use of commercially available donor polymers. The results further indicate that **A1** is a highly promising non-fullerene electron acceptor which offers its suitability with a range of donors, whether conjugated polymers or small molecules, and that the SFX-core is worth examining for futuristic engineering of non-fullerene acceptors.

4. Experimental section

4.1 Materials and methods

All the reactions were carried out under nitrogen atmosphere, unless otherwise stated. Solvents used for various reactions were dried using a commercial solvent purification/drying system. Solvents used for extractions and column chromatography, and all other reagents were used as supplied by commercial vendors without further purifications or drying. 2,2',7,7'-Tetrabromospiro[fluorene-9,9'-xanthene] and 4-methyl-1-octyl-2,6-dioxo-1,2,5,6-tetrahydropyridine-3-carbonitrile were prepared according to the reported literature.[33,46] Thin layer chromatography (TLC) was performed using 0.25 mm thick plates pre-coated with Merck Kieselgel 60 F_{254} silica gel, and visualized using UV light (254 and 365 nm). Petroleum spirits with a boiling point range of 40–60 °C was used wherever indicated. Column chromatography was performed on either 40–60 or 20–40 µm silica gel. 1H NMR spectra were recorded at 300, 400 or 500 MHz, as indicated. The following abbreviations were used to explain multiplicities: s = singlet, d = doublet, t = triplet, q = quartet, m = multiplet, br = broad, dd = doublet of doublets, and dt = doublet of triplets. 13C NMR spectra were recorded at 75 or 101 MHz, as indicated. ^{1}H and ^{13}C chemical shifts were calibrated using residual non-deuterated solvent as an internal reference and are reported in parts per million (δ) relative to tetramethylsilane (δ = 0). PESA measurements were recorded using a Riken Keiki AC-2 PESA spectrometer with a power number of 0.5. Samples for PESA were prepared on ITO cleaned glass substrates and were run using a power setting of 10 nW. TGA experiments were carried out using Q-500 TGA instrument with nitrogen as a purging gas. Samples were heated to 800 °C at a rate of 10 °C per minute under nitrogen atmosphere. Details of spectroscopic measurements, and device fabrication and characterization of photovoltaic devices were reported previously.[36,38,46] Atomic force microscopy topographic maps were directly performed on the active layers of PTB7: **A1** and P3HT: **A1** blends using an Asylum Research MFP-3D-SA instrument. The AFM was run in intermittent contact mode (tapping mode) using MicroMasch NSC18 tips (typical resonant frequency ~100 kHz, typical probe radius ~10 nm and typical aspect ratio 3: 1). TEM samples were prepared by solvent evaporation on a holey carbon grid and micrographs were produced using a JOEL 1010 100 Kv TEM. A Bruker AXS D8 Discover instrument with a general area detector diffraction system (GADDS) using Cu Kα source was utilized to obtain XRD patterns.

4.2 Synthesis

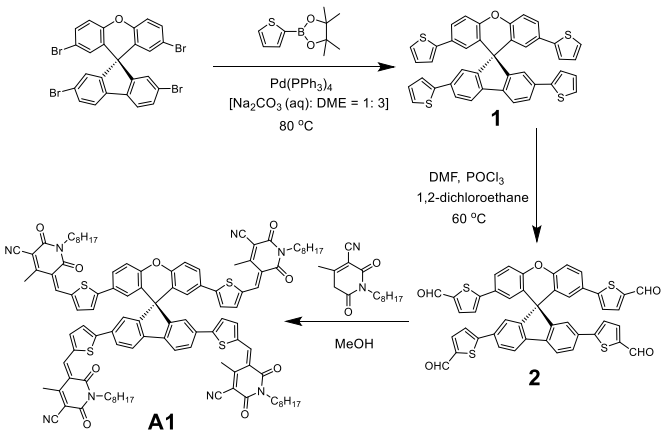

Scheme 1 The synthetic protocol used to synthesize **A1**.

2,2',7,7'-Tetra(thiophen-2-yl)spiro[fluorene-9,9'-xanthene] (1): Compound 2,2',7,7'-tetrabromospiro[fluorene-9,9'-xanthene] (500 mg, 0.772 mmol) was added to a solution of DME: 2M Na_2CO_3 (30 mL) under N_2 followed by addition of 4,4,5,5-tetramethyl-2-(thiophen-2-yl)-1,3,2-dioxaborolane (790 mg, 6.17 mmol). The reaction mixture was degassed under N_2 for 15 minutes and then $Pd(PPh_3)_4$ (17.8 mg, 0.015 mmol) was

added. The resulting mixture was heated at 80 °C for 18 hours and the reaction completion was monitored by TLC. Water (50 mL) was added to the reaction mixture and the aqueous layer was extracted (× 3) with dichloromethane. The combined organic layer was washed with water followed by brine, dried over $MgSO_4$ and concentrated to obtain crude product which was purified using flash chromatography on silica with 40% DCM/hexane mixture as eluent to obtain **1** (450 mg, 88%). ^{1}H NMR (300 MHz, $CDCl_3$) δ 7.81 (d, J = 8.0 Hz, 2H), 7.66 (dd, J = 8.0 Hz, 1.5 Hz, 2H), 7.44–7.49 (m, 4H), 7.29 (d, J = 8.5 Hz, 2H), 7.20–7.24 (m, 4H), 7.08 (dd, J = 4.7 Hz, 1.7 Hz, 2H), 6.98 (dd, J = 5.0 Hz, 3.7 Hz, 2H), 6.87 (dd, J = 7.0 Hz, 2.4 Hz, 4H), 6.72 (d, J = 2.1 Hz, 2H); ^{13}C NMR (75 Hz, $CDCl_3$) δ 117.62, 120.74, 122.90, 122.98, 123.55, 124.45, 124.99, 125.45, 126.42, 126.63, 127.90, 128.11, 130.31, 134.89, 138.69, 143.60, 144.29, 150.90, 155.61; MALDI-TOF (m/z) Calculated for $C_{41}H_{24}OS_4$ $[M]^+$ = 660.07; Found: 660.13.

5,5',5'',5'''-(Spiro[fluorene-9,9'-xanthene]-2,2',7,7'-tetrayl)tetrakis(thiophene-2-carbaldehyde) (2): A solution of $POCl_3$ (0.283 mL, 3.03 mmol) in DMF (0.993 mL, 12.82 mmol) was added to the ice cold solution of compound **1** (200 mg, 0.303 mmol) in 1,2-dichloroethane (10 mL) under N_2 atmosphere. The resultant reaction mixture was stirred at 60 °C. The reaction progress was monitored by TLC. After completion, the reaction mixture was poured onto crushed ice and neutralized with aqueous Na_2CO_3 solution. The aqueous layer was extracted with dichloromethane. The organic layer was separated, washed with brine, dried over $MgSO_4$, and evaporated to obtain crude product which was purified by flash column chromatography using 5% MeOH/DCM eluent to get the titled product (125 mg, 53%). ^{1}H NMR (300 MHz, $CDCl_3$) δ 9.82 (s, 1H), 9.75 (s, 1H), 7.94 (d, J = 8.0 Hz, 2H), 7.79 (dd, J = 8.0 Hz, 1.6 Hz, 2H), 7.65 (d, J = 4 Hz, 2H), 7.55–7.60 (m, 4H), 7.46 (d, J = 1.4 Hz, 2H), 7.34 (dd, J = 11.6 Hz, 6.3 Hz, 4H), 7.04 (d, J = 4 Hz, 2H), 6.71(d, J = 2.2 Hz, 2H); ^{13}C NMR (75 Hz, $CDCl_3$) δ 118.47, 123.44, 123.97, 124.45, 124.71, 126.01, 127.31, 127.42, 129.38, 134.22, 137.29, 137.42, 139.93, 142.29, 151.81, 153.02, 153.40, 155.82, 182.76, 182.79; MALDI-TOF (m/z) Calculated for $C_{45}H_{24}O_5S_4$ = 772.05 $[M]^+$, 795.05 $[M+Na]^+$; Found: 772.11 and 795.11.

(5*Z*,5'*Z*,5''*E*,5'''*E*)-5,5',5'',5'''-((((*S*)-spiro[fluorene-9,9'-xanthene]-2,2',7,7'-tetrayl)tetrakis(thiophene-5,2-diyl))tetrakis(methaneylylidene))tetrakis(4-methyl-1-octyl-2,6-dioxo-1,2,5,6-tetrahydropyridine-3-carbonitrile) (A1): Compounds **2** (100 mg, 0.129 mmol) and cyanopyridone (271 mg, 1.032 mmol) were dissolved in methanol and the resulting mixture was refluxed overnight. Solid thus precipitated in the reaction flask was filtered and was purified using flash chromatography with 1% MeOH/DCM eluent to get the titled product as a cherry solid (82 mg, 36%). ^{1}H NMR (300 MHz, $CDCl_3$): δ 7.99 (s, 4H), 7.85 (s, 2H), 7.77–7.79 (m, 4H), 7.69 (d, J = 3.9 Hz, 2H), 7.58–7.60 (m, 4H), 7.49 (d, J = 3.9 Hz, 2H), 7.42 (d, J = 8.6 Hz, 2H), 7.07 (d, J = 3.5 Hz, 2H), 6.80 (s, 2H), 3.91–3.98 (m, 8H), 2.56 (s, 6H), 2.59 (s, 6H), 1.60 (m, 8H), 1.25–1.29 (m, 48H), 0.87 (t, J = 6.2 Hz, 12H); ^{13}C NMR (75 Hz, $CDCl_3$) δ 14.26, 19.07, 22.79, 27.12, 27.90, 29.32, 29.38, 29.83, 31.93, 31.97 40.59, 54.35, 104.30, 104.57, 114.78, 116.81, 117.15, 118.79, 121.83, 123.81, 124.13, 124.73, 125.46, 126.30, 127.97, 128.27, 129.68, 134.59, 136.88, 137.36, 140.46, 144.39, 146.49, 152.07, 156.49, 158.13, 159.42, 159.42, 159.63, 160.48, 162.94, 163.07; MALDI-TOF (m/z) Calculated for $C_{105}H_{104}N_8O_9S_4$ = 1749.68 $[M+H]^+$, 1771.68 $[M+Na]^+$; Found: 1749.93 and 1771.92, respectively. Elemental analysis calculated for $C_{105}H_{104}N_8O_9S_4$ (%): C 72.05, H 5.99, N 6.40; found C 72.02, H 5.95, N 6.37.

Conflicts of interest

There are no conflicts to declare.

Acknowledgements

S. V. B. acknowledges University Grant Commission (UGC) – Faculty Research Program (India) for providing financial support and an award of professorship. A. G. acknowledges Dr Gerry Wilson from CSIRO Manufacturing, Clayton, Victoria, Australia, for providing support through a visiting fellow position. A. G. is thankful to the Alfred Deakin Fellowship Scheme at the Institute for Frontier Materials (IFM), Deakin University, Waurn Ponds, Victoria, Australia. A. G. would like to thank Australia India Institute (AII), New Delhi, India for providing an Incoming Leader Fellowship Award that enabled him to carry out this very interesting piece of research and also for supporting him with the necessary requirements for this project. A. G. will further acknowledge the assistance of Mr Aman Tyagi, Program Officer at AII, New Delhi. Anuradha., A. A. and A. G. acknowledge various testing and analytical facilities at RMIT University, Deakin University, CSIRO Clayton, and Bio21 Institute, University of Melbourne, Melbourne Victoria, Australia. A. P. acknowledges the use of Gaussian 09 procured under the DST-FIST Scheme (Sanction No. FS/FST/PSI-018/2009). J. Li acknowledges the Australian Research Council (ARC) for support through a Future Fellowship project (FT130100057).

Notes and references

1 G. Yu, J. Gao, J. C. Hummelen, F. Wudl and A. J. Heeger, *Science*, 1995, **270**, 1789.
2 C. J. Brabec, N. S. Sariciftci and J. C. Hummelen, *Adv. Funct. Mater.*, 2001, **11**, 15.
3 F. C. Krebs, *Sol. Energy Mater. Sol. Cells*, 2009, **93**, 394.
4 (*a*) A. J. Heeger, *Chem. Soc. Rev.*, 2010, **39**, 2354; (*b*) L. T. Dou, J. B. You, Z. R. Hong, Z. Xu, G. Li, R. A. Street and Y. Yang, *Adv. Mater.*, 2013, **25**, 6642.
5 S. Li, Z. Zhang, M. Shi, *et al.*, *Phys. Chem. Chem. Phys.*, 2017, **19**, 3440.
6 Z. Liu, Y. Wu, Q. Zhang and x. Gao, *J. Mater. Chem. A*, 2016, **4**, 17604.
7 F. Fernàndez-Làzaro, N. Zink-Lorre and A. Sastre-Santos, *J. Mater. Chem. A*, 2016, **4**, 9336.
8 C. B. Nielsen, *et al.*, *Acc. Chem. Res.*, 2015, **48**, 2803.
9 Y. Lin and X, Zhan, *Mater. Horiz.*, 2014, **1**, 470.
10 S. M. McAfee, J. M. Topple, I. G. Hill and G. C. Welch, *J. Mater. Chem. A*, 2015, **3**, 16393.
11 C. Zhan and J. Yao, *Chem. Mater.*, 2016, **28**, 1948.
12 E. Kozma and M. Catellani, *Dyes Pigm.*, 2013, **98**, 160.
13 R. Y. C. Shin, P. Sonar, P. S. Siew, Z. K. Chen and A. Sellinger, *J. Org. Chem.*, 2009, **74**, 3293.

14 A. Rananaware, A. Gupta, J. Li, A. Bilic, L. Jones, S. Bhargava and S. V. Bhosale, *Chem. Commun.*, 2016, **52**, 8522.
15 H. Patil, W. X. Zu, A. Gupta, V. Chellappan, A. Bilic, P. Sonar, A. Rananaware, S. V. Bhosale and S. V. Bhosale, *Phys. Chem. Chem. Phys.*, 2014, **16**, 23837.
16 A. M. Raynor, A. Gupta, H. Patil, A. Bilic and S. V. Bhosale, *RSC Adv.*, 2014, **4**, 57635.
17 H. Patil, A. Gupta, B. Alford, D. Ma, S. H. Privèr, A. Bilic and S. V. Bhosale, *Asian J. Org. Chem.*, 2015, **4**, 1096.
18 X. F. Wu, W. F. Fu, Z. Xu, M. Shi, F. Liu, H. Z. Chen, J.-H. Wan and T. P. Russell, *Adv. Funct. Mater.*, 2015, **25**, 5954.
19 N. Qiu, H. Zhang, X. Wan, C. Li, X. Ke, H. Feng, B. Kan, H. Zhang, Q. Zhang, Y. Lu and Y. Chen, *Adv. Mater.*, 2017, **29**, 1604964.
20 A. Gupta, A. Rananaware, P. S. Rao, D. D. La, A. Bilic, W. Xiang, J. Li, R. A. Evans, S. V. Bhosale and S. V. Bhosale, *Mater. Chem. Front.*, 2017, **1**, 1600.
21 O. K. Kwon, J.-H. Park, D. W. Kim, S. K. Park and S. Y. Park, *Adv. Mater.*, 2015, **27**, 1951
22 S. Dai, F. Zhao, Q. Zhang, T.-K. Lau, T. Li, K. Liu, Q. Ling, C. Wang, X. Lu, W. You and X. Zhan, *J. Am. Chem. Soc.*, 2017, **139**, 1336.
23 H. Bin, *et al.*, *Nat. Commun.*, DOI: 10.1038/ncomms13651.
24 W. Zhao, *et al.*, *Adv. Mater.*, 2016, **28**, 4734.
25 Y. Lin, *et al.*, *Adv. Mater.*, 2015, **27**, 1170.
26 D. Xie, *et al.*, *Dyes Pigm.*, 2018, **148**, 263.
27 D. Maa, *et al.*, *Dyes Pigm.*, 2018, **150**, 363.
28 G. Zhang, *et al.*, *Chem. Rev.*, 2018, DOI: 10.1021/acs.chemrev.7b00535.
29 Y. Song, S. Lv, X. Liu, X. Li, S. Wang, H. Wei, D. Li, Y. Xiao and Q. Meng, *Chem. Commun.*, 2014, **50**, 15239.
30 H.-W. Luo, *et al.*, *Chin. Chem. Lett.*, 2016, **27**, 1283.
31 N. Liang, *et al.*, *Mater. Chem. Front.*, 2017, **1**, 1291.
32 W. Chen and Q. Zhang, *J. Mater. Chem. C*, 2017, **5**, 1275.
33 M. Maciejczyk, A. Ivaturi and N. Robertson, *J. Mater. Chem. A*, 2016, **4**, 4855.
34 M. Sun, R. Xu, L. Xie, Y. Wei and W. Huang, *Chin. J. Chem.*, 2015, **33**, 815.
35 K. Liu, *et al.*, *Mater. Chem. Front.*, 2017, **1**, 100.
36 A. Rananaware, A. Gupta, G. Kadam, D. D. La, A. Bilic, W. Xiang, R. A. Evans and S. V. Bhosale, *Mater. Chem. Front.*, 2017, **1**, 2511.
37 D. Srivani, A. Agarwal,S. V. Bhosale, A. L. Puyad, W. Xiang, R. A. Evans, A. Gupta and S. V. Bhosale, *Chem. Commun.*, 2017, **53**, 11157.
38 A. Gupta, V. Armel, W. Xiang, G. Fanchini, S. E. Watkins, D. R. MacFarlane, U. Bach and R. A. Evans, *Tetrahedron*, 2013, **69**, 3584.
39 R. J. Kumar, Q. I. Churches, J. Subbiah, A. Gupta, A. Ali, R. A. Evans and A. B. Holmes, *Chem. Commun.*, 2013, **49**, 6552.
40 A. Gupta, A. Ali, T. B. Singh, A. Bilic, U. Bach and R. A. Evans, *Tetrahedron*, 2012, **68**, 9440.
41 M. J. Frisch, *et al.*, *Gaussian 09*, *Revision C.01*, Gaussian Inc., Wallingford CT, 2009.
42 Avogadro: an open-source molecular builder and visualization tool, Version 1.1.0. http://avogadro.openmolecules.net/.
43 M. D. Hanwell, *et al.*, *J. Cheminf.*, 2012, **4**, 17.
44 S. Li, W. Liu, M. Shi, J. Mai, T.-K. Lau, J. Wan, X. Lu, C.-Z. Li and H. Chen, *Energy Environ. Sci.*, 2016, **9**, 604.
45 P. I. Djurovich, *et al.*, *Org. Elect.*, 2009, **10**, 515.
46 A. Gupta, *et al.*, *Chem. Commun.*, 2012, **48**, 1889.